H^- Desorption from Uracil via Metastable Electron Capture

A. Grandi,[1] F. A. Gianturco,[1,*] and N. Sanna[1,2]

[1]*Department of Chemistry, The University of Rome "La Sapienza" and INFM Piazzale A. Moro 5, 00185 Rome, Italy*
[2]*and Supercomputing Center for University and Research, CASPUR, via dei Tizii 6b, 00185 Rome, Italy*

(Received 7 May 2003; published 23 July 2004)

In this Letter we report an analysis of the quantum dynamics for the scattering of slow electrons off uracil molecules, leading to the formation of a trapped, metastable anionic state at around 9 eV of energy. This resonant state is seen to be capable of describing an anionic molecular precursor which can explain the desorption of the H^- species observed in experiments on film deposited uracil samples.

DOI: 10.1103/PhysRevLett.93.048103 PACS numbers: 87.15.Aa, 87.14.Gg

High energy radiation can induce damage in liquids and solids via production of a wide variety of intermediate species that are being formed within nanoscopic volumes along the ionizing tracks. Charged particle track-structure analysis therefore becomes a useful basis for our understanding of the early effects of radiation on matter, especially when one is dealing with biological matter [1–5]. At the elementary level, the formation of a transient negative ion (TNI) by temporary electron attachment to the molecule is followed by energy redistribution via different pathways to dissociative attachment (DA) and dipolar dissociation (DD) that lead in turn to the production of different fragments [5,6]. In order to obtain a more specific understanding of the molecular mechanisms which preside over the above kinetics, one needs to establish a computational and theoretical model which includes, at the quantum level, as much as possible of the above multichannel dynamical process. This procedure is, however, fraught with difficulties and problems, both conceptual and technical, when one decides to set it up for such complicated targets as DNA bases in solution, in thin films or only in the gas phase. In the present example we intend to show the preliminary findings from a nonempirical model for the quantum scattering dynamics of low-energy electrons trapped by the uracil basis. Our model results show that a specific TNI transition state can indicate the energy pathways most likely to be followed by that precursor compound when it fragments. We shall be focusing here on a specific molecular precursor to the desorption of H^- as observed to occur from room temperature thin films of pure uracil condensed on polycrystalline Pt [5]. Other gas-phase studies of this system [7–9] have shown at low energies a broader energy range and a wider pattern of fragmentation products which we have also examined in terms of metastable states and are presented in detail elsewhere [10]. In the present work the total wave function of the "target + e^-" is given as an antisymmetrized product of electronic wave functions which parametrically depend on the positions of the nuclei. Next, the scattering is limited to its elastic part so that for now we restrict our calculation to a single nuclear geometry, this further approximation being commonly referred to as the fixed-nuclei (FN) approximation. The target N electrons are in their ground electronic state which is taken to remain unchanged during the scattering, thereby also disregarding for the moment electronic excitation processes. That state is then described within the Hartree-Fock, self-consistent field (SCF) approximation by using a single determinant of the N occupied molecular orbitals. In our implementation of the scattering equations the occupied molecular orbitals (MOs) of the targets are expanded onto a set of symmetry-adapted angular functions [11–13] with their corresponding radial coefficients represented on a numerical grid.

$$F^{p\mu}(r, \hat{\mathbf{r}} \mid \mathbf{R}) = \sum_{l,h} r^{-1} f_{lh}^{pu}(r \mid \mathbf{R}) X_{lh}^{p\mu}(\hat{\mathbf{r}}), \qquad (1)$$

where we refer to the μth element of the pth irreducible representation (IR) of the point group of the molecule at the nuclear geometry R. The angular functions $X_{lh}^{p\mu}(\hat{\mathbf{r}})$ are symmetry adapted angular functions given by proper combination of spherical harmonics $Y_{lm}(\hat{\mathbf{r}})$, the coefficients of which have been often discussed in the literature [10–13]. We have treated correctly the target molecule symmetry (C_s) while increasing the symmetry of the scattered electron to D_{2h}. This technical artifice reduced the computational cost of solving the coupled channel scattering equations without substantially altering final results (for a more extended discussion see, Ref. [10]) The bound molecular electrons are given by the $D95^{**}$ basis set expansion over Gaussian-type functions (GTO's). The quantum scattering equations take the familiar form [14]

$$\left[\frac{d^2}{dr^2} - \frac{l(l+1)}{r^2} + 2(E - \epsilon_\alpha)\right] f_{lh}^{p\mu\alpha}(r \mid \mathbf{R}) = \sum_{l'h'\beta'} \int dr' V_{lh,l'h'}^{p\mu,\alpha\beta}(r, r' \mid \vec{R}) f_{l'h'}^{p\mu,\beta}(r' \mid \mathbf{R}), \quad (2)$$

where E is the collision energy $E = k^2/2$ and ϵ_α is the electronic eigenvalue for the αth asymptotic state. The $|p\mu\rangle$ indices label the specific μth component of the pth IR that belongs to the αth electronic target state (initial state) coupled with the infinity of excited state IR's

labeled collectively by β. Equations (2) contain the kernel of the integral operator V, a sum of diagonal and nondiagonal terms that fully describe the electron-molecule interaction during the collision. To further truncate the sum on the right-hand side of Eq. (2) to a single state α obtains the exact-static-exchange (ESE) representation of the electron-molecule interaction for the chosen electronic target state (ground state) at the nuclear geometry $\mathbf{R}$. In case of choosing a local e^- molecule exchange interaction [14]

$$\left[\frac{d^2}{dr^2} - \frac{l_i(l_i+1)}{r^2} + k^2\right] f_{ij}^{p\mu}(r \mid \mathbf{R}) = \sum_n V_{in}^{p\mu}(r \mid \mathbf{R}) f_{nj}^{p\mu}(r \mid \mathbf{R}), \quad (3)$$

where the indices i, j, or n represent the "angular channel" $|lh\rangle$ and the potential coupling elements are given as

$$V_{in}^{p\mu}(r \mid \mathbf{R}) = \langle X_i^{p\mu}(\hat{\mathbf{r}}) \mid V(\mathbf{r} \mid \mathbf{R}) \rangle | X_n^{p\mu}(\hat{\mathbf{r}}) \rangle = \int d\hat{\mathbf{r}} X_i^{p\mu}(\hat{\mathbf{r}}) V(\mathbf{r} \mid \mathbf{R}) X_n^{p\mu}(\hat{\mathbf{r}}). \quad (4)$$

The standard Green's function technique allows us to rewrite the previous differential equations in an integral form:

$$f_{ij}^{p\mu}(r \mid \mathbf{R}) = \delta_{ij} j_{l_i}(kr) + \sum_n \int_0^r dr' g_{l_i}(r, r') V_{in}(r' \mid \mathbf{R}) f_{nj}^{p\mu}(r' \mid \mathbf{R}). \quad (5)$$

The integral on the right-hand side of Eq. (5) terminates at $r' = r$ and Eqs. (5) are recognized as Volterra-type equations [15,16]. We replace the nonlocal exchange with an energy-dependent local potential, as suggested by Hara [17] within the free-electron gas model (HFEGE):

$$V_{ex}^{\mathrm{HFEGE}}(\mathbf{r}) = \frac{2}{\pi} k_F(\mathbf{r}) \left(\frac{1}{2} + \frac{1-\eta^2}{4\eta} \ln \left| \frac{1+\eta}{1-\eta} \right| \right), \quad (6)$$

where $\eta(\mathbf{r}) = (k^2 + 2I_p + k_F)^{1/2}/k_F, k_F(\mathbf{r}) = [3\pi^2 \rho(\mathbf{r})]^{1/3}$ is the local Fermi momentum and I_p is the ionization potential of the molecular target [11–14].

For a realistic description of the e^--molecule interaction we need to calculate not only electronic excitations but also the virtual excitations of bound electrons, i.e., the effect of static and dynamic bound-continuum electron correlation. We therefore additionally included the effects of dynamical correlation and polarization through a local energy-independent potential V_{cp}. The V_{cp} model potential contains a short-range correlation contribution, V_{corr}, which is smoothly connected to a long-range polarization contribution, V_{pol}. The short-range term is obtained by defining an average dynamical correlation energy of a single electron within the formalism of Kohn and Sham variational theorem [14]. The functional derivative of such as quantity with respect to the SCF N-electron density of the molecular target provides a density functional description of the required short-range correlation term as an analytic function of the target electron density. The long-range part of V_{cp} asymptotically agrees with the potential $-\alpha/2r^4$ (α is a static dipole polarizability of the target in its ground electronic state: its value in the case of Uracil was of 68.1 a_0^3). This corresponds to including the dipole term in the second-order perturbation expansion of the polarization potential. The largest angular momentum employed to describe the SCE (C_s symmetry) potential expansion was $L_{\max} = 80$, while $l_{\max} = 40$ was used for the scattering partial wave expansion. The total numerical grid in (r, ϑ, φ) was given by $1300 \times 84 \times 324$ points and the number of coupled equations for each of the IR describing the scattering states was more than 6000. The symmetry of the scattered electron as mentioned before was taken to belong to the D_{2h} point group.

The experiments [5] carried out electron-stimulated desorption of H^- from prepared thin films of pure uracil that had been condensed on a polycrystalline Pt substrate. Comparison with gas phase measurements [7,18] had suggested that the H^- desorbed from the thin films was mainly the result of CH bond cleavage producing that strong desorption peak around 9 eV, a feature not observed at such low mass in the gas phase experiments [7–9] that focused instead on the lower energy region of the DA product fragmentation and on low-energy electron current transmission spectra [19]. We shall see below that the present calculation qualitatively confirms that desorption picture and further pinpoints the structure of the formed resonant state. Figure 1 reports the partial cross sections obtained from our calculations for the scattering states which contribute the most to the elastic integral cross sections. The b_{1g} contribution, given by a thick line, clearly shows a marked peak centered at 9.07 eV. The

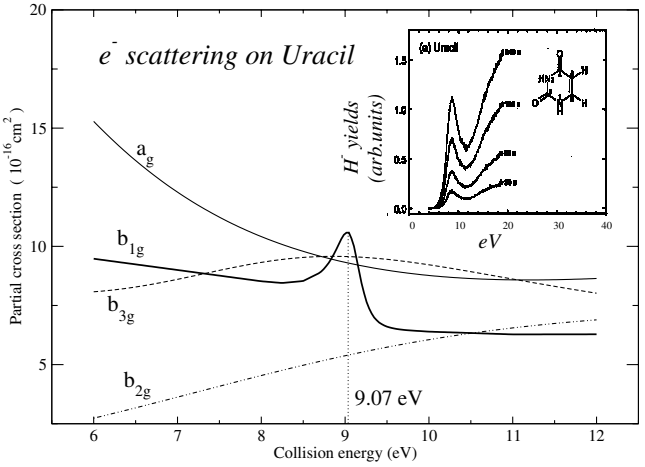

FIG. 1. Computed partial integral cross sections for electron scattering from gas-phase uracil. Inset: experimental H^- desorption from Ref. [5].

inset reports the experimental results from Ref. [5], showing the chemical formula, and the atom numbering of the uracil molecule. The uncertainty in the measured absolute peak position electron energy is about ± 0.25 eV and the peaks appear at 8.7 eV [5]. It is clear from the comparison that the computed position of our resonance is fairly close to measurements: we shall discuss below why the corresponding width of our computed resonance is here narrower than the fairly broad experimental width of the desorption peaks [5,18]. Figure 2 reports the computed eigenphase sum: it essentially represents the multichannel equivalent of the phase shift of each separate partial wave appearing in a potential scattering treatment [20] and it describes the global effects of a strongly anisotropic potential (as in our case) on the deflection and trapping of the scattered electron. The marked rise around 9 eV by about π radians points at the existence of a shape resonance since no other dynamical resonant channel can exist in the present model. We see from our calculations that the actual location of the resonance depends on the number of partial waves employed to describe the scattered electron. The three different choices in the figure are seen to shift its half-maximum location, although to increase $l_{\max}$ up to 40 [i.e., solving 6561 coupled equations over the several thousand points of the (r, ϑ, φ) grid] moves that resonance by 0.2 eV only and therefore does not affect much the qualitative picture extracted from calculations, while, however, helping in explaining the marked differences found between computed and measured width values: our lack of nuclear dynamics and of convergence saturation could account for only a qualitative agreement between computed and measured resonance shapes. Given the complexity of the numerics involved in solving such a huge set of equations, we felt that there was no real need to extend further the convergence study for the present model dynamics. When the above quantity is fitted with a quadratic Wigner formula [20], the position of the resonant state is at 9.07 eV, with a width of 0.38 eV. It corresponds to a resonance lifetime about 1.25×10^{-14} s which is already about 100 times longer than the interaction time between the scattered electron and the target molecule for a direct collision at the same energy. If one further considers that the vibrational times of the several normal modes existing for the uracil molecule range between 10^{-15} and 10^{-12} s [21], then we see that the above resonant state, although decaying rather rapidly (as explained above) still lives longer than the vibrational modes associated to the CH stretching motion. Finally, the inset of Fig. 2 shows that the dominant contribution to the found TNI comes from the $\ell = 4$ partial wave, a feature which suggests the presence of several nodal planes in the scattered electron wave function.

We report in Fig. 3 our calculations for the lower-lying virtual molecular orbitals (MOs) obtained from SCF calculations at the equilibrium geometry of uracil (U) and for the relaxed geometry of the stable negative ion uracil$^-$ (U$^-$) both computed at the correct C_s symmetry. The relaxation effect caused by the stable negative ion formation is seen by the energy shift occurring between the lowest unoccupied molecular orbital (LUMO) of U and the highest occupied molecular orbital (HOMO) of U$^-$. The location of several, metastable MOs is shown for the U system and we have highlighted the one corresponding to the location of our resonant state. That specific unoccupied MO (UMO) is the 9th in the sequence of them and indeed shows a spatial symmetry close to that of the scattering state: (b_{1g}). In order to further stress the pictorial value of this finding, we report on the right part of the figure a probability density map of that UMO over the space of the atomic nuclei of the ground state of the uracil molecule. The virtual MO clearly shows a marked

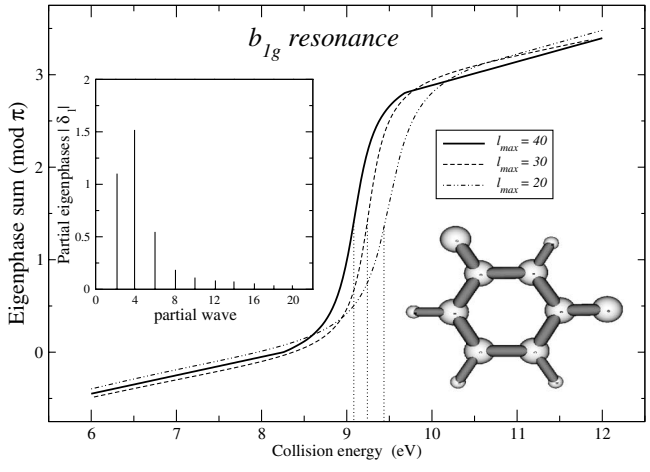

FIG. 2. Scattering eigenphase sum of b_{1g} symmetry (see text for details) as a function of collision energy and for three different partial wave expansions of the scattered electron. The inset shows the individual coefficients as a function of the partial wave contributions.

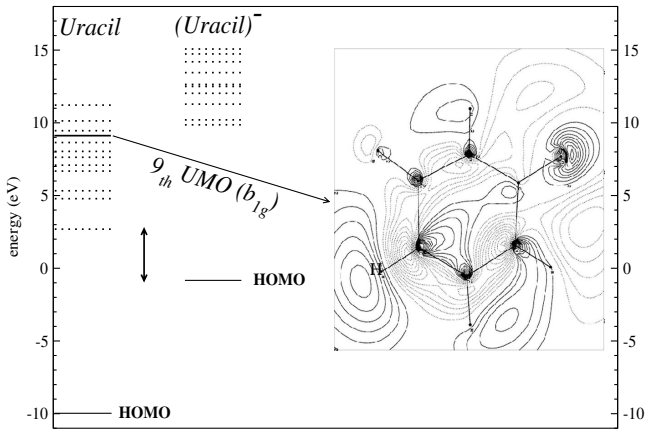

FIG. 3. Highest occupied molecular orbitals (HOMO's) and virtual orbitals (UMO's) of uracil and of uracil negative ion. The map of the inset shows the excess electron density distribution for the virtual orbital selected on the left of the figure.

electron density increase on the H atom attached to the C_5 atom of the uracil ring, the very one considered by experiments to be involved in the H^- desorption process [5]. It also shows that one of its nodal planes cuts across that same C-H bond, indicating clear antibonding character of the added electron density along that bond: the latter is therefore more likely to break up during the extra electron energy release into the molecular nuclear network. We also see that the energy involved in the rearrangement process from ground state U into ground state U^- (without zero point energy corrections) is around 3 eV, i.e., much less than the 9.0 eV available after electron trapping into the UMO shown in the figure. This means, at least qualitatively, that the TNI species formed under near-Franck-Condon conditions during the resonant scattering can release several eV of energy by relaxation into the molecular nuclear motions, thereby very likely causing the dissociative effects along one of the multidimensional components of the vibrational network of the molecule. Our calculations show the additional electron density to be chiefly located onto one specific H atom, i.e., the one bound to the C_5 atom, and exhibiting antibonding character across that bond: they thus suggest that the extra energy of the TNI species could be preferentially funneled into a DA channel where the C_5–H^- bond breaks up, thereby releasing the H^- fragments. One should keep in mind, however, the preliminary nature of the present model study and to understand it within the general context of the many qualitative discussions appearing in the experimental reports [7–9,18,19] which indeed point out that at such electron energies the higher molecular electronic states are expected to be strongly coupled to the ground state and would also therefore give rise to Feshbach or core-excited resonances: the latter would then modify possible shape resonances both in their widths and positions. We argue here that the finding of a marked, fairly long-lived, shape resonance from our nonempirical scattering calculations suggests the strong possibility that such a state would also survive when further electronic and nuclear dynamical effects were to be added to the quantum scattering and that the corresponding excess electron density over the molecule would still be guided by the existence of specific antibonding features as those shown by our calculations.

The present study has therefore shown the presence of what could be called a ''precursor'' resonant state above the energy of the stable U^- formation and found it to be positioned in energy close to the experimentally observed H^- production [5]. We have further shown that this resonant TNI could be described by our simple model as being due to the initial trapping of the extra electron behind the $l = 4$ centrifugal barrier and as having several nodal planes in its spatial wave function. The analysis of the associated MO indicates that the extra electron is chiefly located on the H atom bound to the C_5 carbon of the uracil ring and it exhibits antibonding character across that C-H bond. Hence, one can conjecture that the extra energy carried by the resonant electron, once coupled to the molecular vibrational modes, will lead to several possible DA processes and that the one causing the breaking of that C-H bond, with the ensuing release of the H^- fragment, could become favored in the present system due to the specific density features of the resonant electron and the environmental effects (thin films) on the molecular target.

The support of the University of Rome ''La Sapienza'' Research Committee and of the CASPUR computational facilities are here gratefully acknowledged.

*Corresponding author.
Email address: fa.gianturco@caspur.it

[1] M. Inokuti, Radiat. Eff. Defects Solids **117**, 143 (1991).
[2] S. Denifl, S. Ptasinka, M. Cingel, S. Matejcik, P. Scheier, T. D. Maerk, Chem. Phys. Lett. **377**, 74 (2003).
[3] B. Boudaiffa, P. Cloutier, D. Hunting, M. A. Huels, and L. Sanche, Science **287**, 1658 (2000).
[4] H. Abdoul-Carime, M. A. Huels, L. Sanche, F. Bruenig, and E. Illenberg, J. Chem. Phys. **113**, 2517 (2000).
[5] M.-A. Hervé du Penhoat, M. A. Huels, P. Cloutier, J.-P. Jay-Gerin, and L. Sanche, J. Chem. Phys. **114**, 5755 (2001).
[6] C. von Sonntag, *The Chemical Basis of Radiation Biology* (Taylor & Francis, London, 1987).
[7] G. Hanel, B. Gstir, S. Denife, P. Scheier, M. Probst, B. Farizon, M. Farizon, E. Illenberger, and T. D. Maerk, Phys. Rev. Lett. **90**, 188104 (2003).
[8] M.-A. Hervé du Penhoat, M. A. Huels, P. Cloutier, J.-P. Jay-Gerin, and L. Sanche, Phys. Chem. Chem. Phys. **5**, 3270 (2003).
[9] S. Denifl, S. Ptasinka, G. Hanel, B. Gstir, M. Probst, P. Scheier, and T. D. Maerk, J. Chem. Phys. **120**, 6557 (2004).
[10] F. A. Gianturco and R. R. Lucchese, J. Chem. Phys. **120**, 7446 (2004).
[11] R. R. Lucchese and F. A. Gianturco, Int. Rev. Phys. Chem. **15**, 429 (1996).
[12] F. A. Gianturco and R. R. Lucchese, J. Phys. B **29**, 3955 (1996).
[13] F. A. Gianturco and R. R. Lucchese, J. Chem. Phys. **111**, 6769 (1999).
[14] For details, see E. A. Gianturco and A. Jain, Phys. Rep. **143**, 347 (1986).
[15] E.g., see W. N. Sams and D. J. Kouri, J. Chem. Phys. **51**, 4815 (1969).
[16] R. Curik, F. A. Gianturco, and N. Sanna, J. Phys. B **33**, 615 (2000).
[17] S. Hara, J. Phys. Soc. Jpn. **22**, 710 (1967).
[18] H. Abdoul-Carime, M. A. Huels, E. Illenberg, and L. Sanche, J. Am. Chem. Soc. **123**, 5354 (2001).
[19] A. M. Scheer, K. Aflatooni, G. A. Gallup, and P. D. Burrow, Phys. Rev. Lett. **92**, 068102 (2004).
[20] E.g., see C. J. Joachain, *Quantum Collision Theory* (North Holland Publ. Co., Amsterdam & Oxford, 1975), Chap. 3.
[21] J. Lorentzon, M. P. Fulscher, and B. O. Roos, J. Am. Chem. Soc. **117**, 9265 (1995).